EQCM Studies of the Redox Processes during and after Electropolymerization of Films of Transition-Metal Complexes of Vinylterpyridine

Kazutake Takada,[†] Gregory D. Storrier,[†] Félix Pariente,[‡] and Héctor D. Abruña*[,†]

Department of Chemistry, Baker Laboratory, Cornell University, Ithaca, New York 14853-1301, and Departmento de Química Analítica y Análisis Instrumental, Universidad Autónoma de Madrid, Canto Blanco 28049, Madrid, Spain

Received: June 6, 1997; In Final Form: October 7, 1997

The electropolymerization of the transition-metal complexes $[M(v\text{-}tpy)_2]^{n+}$ (M = Fe^{II}, Ru^{II}, Os^{II}, Cr^{III}, Co^{II}, Ni^{II}; v-tpy = 4′-vinyl-2,2′:6′,2″-terpyridine) and the redox processes of their electropolymerized films have been investigated in acetonitrile solution using the electrochemical quartz crystal microbalance (EQCM) and admittance measurements of the quartz crystal resonator. From changes in the frequency, polymerization for each of the complexes was found to be initiated by reduction of the ligand (v-tpy) except for $[Ni(v\text{-}tpy)_2]^{3+}$, where the mechanism appears to involve an ostensibly metal-centered reduction. In all cases, the increase in the resistance parameter of the electrical equivalent circuit of the resonator with potential cycling also indicated polymerization onto the electrode surface. The redox processes of the polymerized $[M(v\text{-}tpy)_2]^{n+}$ films appear to be of the anion-exchange type with changes in the film morphology. A mechanism for the "charge-trapping" process of a uniform coating of poly-$[M(v\text{-}tpy)_2]^{2+}$ (M = Fe, Ru, Os) is proposed in terms of changes in film morphology.

Introduction

The electropolymerization of vinyl-substituted pyridine and polypyridine complexes of transition metals has provided one of the most versatile routes for the modification of electrode surfaces with redox-active films of the monomer complexes. The fact that the surface coverage (Γ) can be controlled from submonolayer amounts to multilayer equivalents has allowed for a number of studies of the physicochemical properties of these films to be explored as a function of Γ.

Since the initial report by Murray and co-workers[1] on electropolymerization of 4-vinylpyridine (v-py) and 4-vinyl-4′-methyl-2,2′-bipyridine (v-bpy) complexes, a vast number of complexes of these and related materials have been prepared and studied.[2−9] Similar to v-py and v-bpy, electrochemical reduction of $[M(v\text{-}tpy)_2]^{n+}$ (M = Fe^{II}, Ru^{II}, Os^{II}, Cr^{III}, Co^{II}, Ni^{II}; v-tpy = 4′-vinyl-2,2′:6′,2″-terpyridine) complexes gives rise to electroactive polymer films of the monomers onto electrode surfaces.[10−14] Electrodes modified with electropolymerized films of $[M(v\text{-}tpy)_2]^{n+}$ complexes have been used to investigate electrochemical characteristics such as electron transfer and charge propagation kinetics.[11,14] We have also reported on the electrocatalytic activity of electropolymerized film of $[Co(v\text{-}tpy)_2]^{2+}$, $[Fe(v\text{-}tpy)_2]^{2+}$, and $[Ni(v\text{-}tpy)_2]^{2+}$ complexes toward the reduction of CO_2 and O_2.[11−13,15,16] Most recently, we showed that electropolymerized films of $[Cr(v\text{-}tpy)_2]^{3+}$ are very active in the electrocatalytic reduction of nitric oxide.[14]

The studies of Murray and co-workers have primarily emphasized electropolymerization of v-bpy complexes (e.g., $[M(v\text{-}bpy)_3]^{2+}$, M = Ru, Fe, Os), whose structures are quite similar to those of the corresponding $[M(v\text{-}tpy)_2]^{2+}$ complexes.[1,2,17,18] As part of those studies, they reported on an especially interesting effect in bilayer films (for example, poly-$[Ru(bpy)_2(v\text{-}py)_2]^{2+}$ and poly-$[Ru(v\text{-}bpy)_2pyCl]^{+}$ or poly-$[Ru(v\text{-}bpy)_3]^{2+}$ and PVF (polyvinylferrocene) for inner and outer films, respectively) which they referred to as "charge trapping".[1,2,17,18] Charge trapping is a phenomenon that arises for spatially segregated bilayer films on electrode surfaces where electronic communication of the outer film with the electrode is inhibited (due to the distance separating the two) so that the outer film's redox reactions are mediated by the inner film. This gives rise to very sharp current peaks that typically occur at the leading edge of voltammetric waves for the inner film. The current flow is unidirectional or rectifying, similar to that at interfaces between semiconductor materials. A similar charge-trapping effect has also been observed for films formed from a single type of monomer by a number of researchers.[7] Although in this case the mechanism of charge trapping has not been clarified, it is believed to arise, at least in part, from redox centers that are electronically isolated from the surface so that their redox reactions are mediated by adjacent redox sites in a manner that is qualitatively similar to that in bilayer films.

In this paper, we present studies on the electropolymerization processes of the metal complexes $[M(v\text{-}tpy)_2]^{n+}$ (M = Fe^{II}, Ru^{II}, Os^{II}, Cr^{III}, Co^{II}, Ni^{II}) in acetonitrile (AN) solution from two viewpoints. First, we studied changes in mass and morphology of the film depositing onto the electrode surface by means of the electrochemical quartz crystal microbalance (EQCM) technique and, second, admittance (impedance) measurements of the quartz crystal resonator on the basis of the electrical equivalent circuit analysis. Further, since electrodes modified with electropolymerized films (henceforth referred to simply as films) of $[M(v\text{-}tpy)_2]^{2+}$ (M = Fe, Ru, Os) in AN were found to exhibit "charge-trapping" behavior, we have also investigated its mechanism, as well as their mass-transfer processes using the above-mentioned techniques.

[†] Cornell University.
[‡] Universidad Autónoma de Madrid.
* To whom correspondence should be addressed.

S1089-5647(97)01860-9 CCC: $15.00
Published on Web 01/30/1998

Experimental Section

Materials. The ligand 4′-vinyl-2,2′:6′,2″-terpyridyl (v-tpy) and its metal complexes were prepared according to literature methods.[10−12,15] AN (Burdick and Jackson distilled in glass) was dried over 4 Å molecular sieves for at least one month before use. Tetra-*n*-butylammonium perchlorate (TBAP) (G.F.S. Chemicals) was recrystallized three times from ethyl acetate and dried under vacuum for 96 h. All other reagents (analytical grade) were used without further purification.

Apparatus. AT-cut quartz crystals (5 MHz) of 24.5 mm diameter with Pt electrodes deposited over a Ti adhesion layer (Maxtek) were used for EQCM measurements. An asymmetric keyhole electrode arrangement was used, in which the circular electrodes' geometrical areas were 1.370 cm^2 (front side) and 0.317 cm^2 (backside). The electrode surfaces were overtone polished, giving rise to smooth surfaces. The quartz crystal resonator was set in a probe (TPS-550, Maxtek) made of Teflon, and in which the oscillator circuit was included. The probe was connected to a homemade conventional three-compartment electrochemical cell by a Teflon joint. The quartz crystal was held vertically. One of the electrodes of the quartz crystal resonator, in contact with the solution, was also used as the working electrode in electrochemical experiments. The potential of the working electrode was controlled with a potentiostat (CV-27, BAS). A sodium chloride saturated calomel electrode (SSCE) and a coiled Pt wire were used as reference and counter electrodes, respectively, unless otherwise noted. The frequency response, measured with a plating monitor (PM-740, Maxtek), and the current, measured with the potentiostat, were simultaneously recorded by a personal computer that was interfaced to the above instruments using LabView (National Instruments). The admittance of the quartz crystal resonator was measured near its resonant frequency by an impedance analyzer (HP4194A, Hewlett-Packard) equipped with a test lead (HP16048A). A probe similar to the one used in the EQCM measurements, but which did not include an oscillator circuit inside, was used to accomplish a direct connection of the quartz crystal resonator to the impedance analyzer.

Procedures. The quartz crystal resonator was cleaned prior to use by continuous cycling between −0.2 and +1.2 V vs Ag/AgCl in a 0.10 M H_2SO_4 solution until the voltammetry of a clean polycrystalline platinum electrode was obtained. The quartz crystal was washed with water and acetone and dried in air for 30 min. Electropolymerization of the complexes was carried out in 0.1 M TBAP/AN as previously described.[10−12,15] Solutions for electropolymerization were typically 0.5 mM in the redox species and were degassed by purging with prepurified nitrogen, which was also passed through oxygen (Oxysorb) and hydrocarbon traps, for at least 15 min. After polymerization, the modified quartz crystal electrode was thoroughly rinsed with AN and subsequently transferred to a pure supporting electrolyte (0.10 M TBAP/AN) solution and allowed to equilibrate for at least 30 min. The surface coverages were determined from integration of the area under the voltammetric waves (at low sweep rates) for the metal-based redox processes.

Results and Discussion

Electropolymerization. The electropolymerization of $[M(v\text{-}tpy)_2]^{n+}$ complexes is believed to proceed via radical−radical coupling of the vinyl moieties[10,11,13] in a fashion similar to v-bpy complexes.[1,3,4] Electropolymerization requires reduction of the v-tpy ligands, whose redox potentials in $[M(v\text{-}tpy)_2]^{n+}$ complexes are generally in the range of −1.2 to −1.7 V vs SSCE. We have recently reported the formal potentials for films of $[M(v\text{-}tpy)_2]^{n+}$ complexes deposited on glassy carbon electrodes in a 0.1 M TBAP/AN solution, and the values are quite similar to those in solution, suggesting that there are no significant changes during the electropolymerization process.[13]

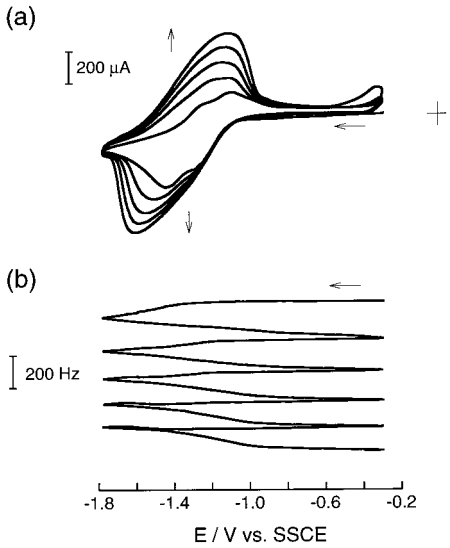

Figure 1. Typical cyclic voltammogram (a) and frequency−potential curve (b) for a quartz crystal electrode (Pt) in a 0.10 M TBAP acetonitrile (AN) solution containing 0.5 mM $[Fe(v\text{-}tpy)_2](PF_6)_2$ at 100 mV s^{-1} (five consecutive scans).

Since details of the EQCM technique have been previously described in a number of reviews,[19,20] only a brief description is given here. A decrease or increase in the frequency of a quartz crystal usually indicates mass loading onto or unloading from the quartz crystal, respectively.[21] However, since changes in frequency are caused not only by changes in mass but also by changes in solution properties, such as viscosity and density,[22−24] and film properties, such as viscoelasticity,[25,26] roughness,[27−30] thickness,[19,25,31,32] and solvophilicity of the film in contact with the quartz crystal resonator, the main factors giving rise to changes in frequency upon electropolymerization of the $[M(v\text{-}tpy)_2]^{n+}$ complexes onto the quartz crystal resonator need to be confirmed. To check for changes in these properties, admittance measurements of the quartz crystal resonator are informative. Admittance measurements are generally carried out using an impedance analyzer from which the resistance parameter of the electrical equivalent circuit for the quartz crystal resonator can be evaluated. Since the resistance parameter, which is given as the reciprocal of the maximum conductance for an ideal system, corresponds to a loss of mechanical energy dissipated to the surrounding medium, any changes in the film properties will result in a change in the resistance parameter.[19,25,32−34] Therefore, an increase in the resistance parameter usually indicates an increase in the viscoelasticity, roughness, or solvophilicity of the film or decrease of the film's thickness on the quartz crystal resonator, whereas a decrease in the resistance parameter indicates a decrease in those properties or an increase in the film's thickness.

Using the EQCM technique along with admittance measurements, we have studied the behavior during and after electropolymerization of $[M(v\text{-}tpy)_2]^{n+}$ complexes at a Pt electrode surface, and the results are presented herein.

$[M(v\text{-}tpy)_2]^{2+}$ (M = Fe, Ru, Os). Because of their overall similarity in behavior, these three materials are considered together as a group. Figure 1 shows (a) the typical current (cyclic voltammogram, CV) and (b) frequency responses as a function of applied potential between −0.30 and −1.80 V at

100 mV s^{-1} for an electrode in contact with a 0.10 M TBAP/AN solution containing 0.5 mM $[Fe(v\text{-}tpy)_2](PF_6)_2$. The same overall tendencies in responses (both current and frequency) were obtained at a sweep rate (υ) of 10 mV s^{-1}, suggesting that, at least for these complexes, qualitatively the responses obtained were independent of the sweep rate. The waves, which in the initial voltammetric scan were centered at −1.24 and −1.41 V vs SSCE, correspond to ligand-based redox processes. The increase in current with continuous potential scanning indicates the accumulation of an electroactive film on the electrode surface. The overall decrease in frequency upon continuous potential scanning also demonstrates that polymerization of the $[Fe(v\text{-}tpy)_2]^{2+}$ complex is taking place on the electrode surface. It should be noted that on the first scan the frequency decreased during the cathodic sweep from ca. −1.1 V and continued to decrease gradually even after scan reversal and at potentials where the v-tpy ligands are ostensibly no longer reduced. These observations indicate that polymerization is initiated only when the applied potential is within the range where vinylterpyridine is reduced. However, once polymerization is initiated, it appears to propagate even after the applied potential is reversed, although this continued increase in mass during oxidation of the reduced film probably also reflects incorporation of perchlorate anion into the film. There may also be changes in solvation and film morphology such as rigidity, which could also affect the frequency response.

We have additional EQCM evidence that suggests that electropolymerization continues even after scan reversal and at potentials where the v-tpy ligands should not be reduced. A cathodic scan at 10 mV s^{-1} was initiated at −0.3 V, and the potential reversed at −1.8 V. At −1.1 V (which corresponds to a potential that is about 100 mV positive of the formal potential for the first v-tpy based reduction) the sweep was arrested. The current decreased rapidly and reached a steady-state value of ca. −10 μA. The frequency decreased rapidly immediately after the potential sweep was arrested and then decreased linearly and continuously at a rate of ca. −22 Hz s^{-1} for 30 s. Since the number of redox active sites within the film is limited, if the decrease in frequency were only due to the incorporation of anions and/or solvent molecules upon oxidation of the v-tpy, the changes should reach zero. Further, if the decrease in frequency was caused only by changes in film morphology, no cathodic current should flow as such changes would not involve Faradaic reactions. Therefore, we conclude that electropolymerization continues to take place even at potentials where the v-tpy is ostensibly not reduced. It should also be mentioned that if the potential was held at −1.1 V on the initial cathodic sweep (i.e., without going out to −1.8 V), there was no evidence of polymerization, suggesting that the polymerization process is initiated at these more negative potentials where the v-tpy is reduced.

As the number of scans increased, reduction from ca. −1.5 V caused a slight increase in the frequency followed by a decrease. Since the film's thickness increases with successive scanning, the increase in frequency is likely due to the ejection of anions and/or solvent molecules from the film upon reduction to maintain charge neutrality (and appropriate solvation) within the film while the decrease in frequency is caused by accumulation of the polymer film on the electrode. Unfortunately, since the resistance parameter of the electrical equivalent circuit for the quartz crystal resonator increased by about 3 Ω upon polymerization during even a single potential cycle over the range from 0 to −1.8 V at 100 mV s^{-1}, it was difficult to calculate the changes in mass due to polymerization. A detailed analysis of the impedance behavior and changes in the resistance parameter will be presented below.

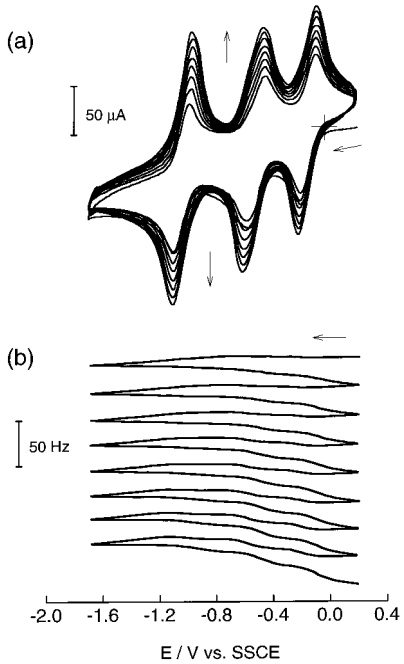

Figure 2. Typical cyclic voltammogram (a) and frequency−potential curve (b) for a quartz crystal electrode (Pt) in a 0.10 M TBAP/AN solution containing 0.5 mM $[Cr(v\text{-}tpy)_2](PF_6)_3$ at 100 mV s^{-1} (seven consecutive scans).

Similar to $[Fe(v\text{-}tpy)_2]^{2+}$, the CV response of $[Ru(v\text{-}tpy)_2]^{2+}$ (at a concentration of about 0.5 mM) between −0.50 and −1.75 V in a 0.10 M TBAP/AN solution exhibited two waves centered at −1.21 and −1.43 V corresponding to v-tpy-based redox processes, which grew with continuous potential scanning, indicating accumulation of an electroactive polymer film onto the electrode surface. An overall decrease in frequency with potential scanning, in a fashion similar to $[Fe(v\text{-}tpy)_2]^{2+}$, was also consistent with the electropolymerization of $[Ru(v\text{-}tpy)_2]^{2+}$ on the electrode surface. Further, the film exhibited changes in frequency analogous to those observed for $[Fe(v\text{-}tpy)_2]^{2+}$. On the first cathodic scan the frequency began to decrease from ca. −1.25 V and continued to decrease even after potential reversal. Afterward, and with continuous potential scanning, the frequency increased slightly upon reduction from around −1.3 V followed by a relatively large decrease at more negative potentials. These frequency changes are ascribed to the same processes described above for $[Fe(v\text{-}tpy)_2]^{2+}$.

The electropolymerization of $[Os(v\text{-}tpy)_2]^{2+}$ exhibited behavior that was qualitatively the same as that described above for both $[Fe(v\text{-}tpy)_2]^{2+}$ and $[Ru(v\text{-}tpy)_2]^{2+}$. However, in this case the ligand-based redox processes were at −1.16 and −1.42 V, consistent with the presence of osmium as the metal center. The similarity among the observed properties for the Fe, Ru, and Os complexes was anticipated due to the negligible effect that the metal centers have on the ligand-based reduction potentials.

$[Cr(v\text{-}tpy)_2]^{3+}$. Figure 2 shows (a) the CV and (b) the frequency−potential curve between +0.20 and −1.70 V for an electrode in contact with a 0.10 M TBAP/AN solution containing 0.5 mM $[Cr(v\text{-}tpy)_2](PF_6)_3$. As illustrated in the CV, this complex exhibits three sets of voltammetric waves at formal potential values of −0.16, −0.54, and −1.06 V, corresponding to Cr localized (Cr(II/I) and Cr(I/0)) and Cr/ligand localized redox reactions, respectively.[13,35] There is also an additional

metal-based Cr(III/II) process at significantly more positive potentials, but since the initial potential was set at +0.2 V, where the metal center exists as the Cr(II) state and the scans were in the negative direction, this last redox process was not observed. The complex also exhibits additional ligand-localized reductions at significantly more negative potentials (−1.76 and −1.95 V; not shown). Analogous to the other materials described above, $[Cr(v\text{-}tpy)_2]^{3+}$ exhibited an increase in the current with consecutive potential cycling with a concomitant overall decrease in frequency indicative of the formation of an electroactive film on the electrode (Figure 2b).

On the initial negative scan, the frequency increased slightly upon reduction from −0.25 to −0.70 V and then decreased during continuous cathodic scanning. The origin of this initial increase in frequency, which was not observed for $[M(v\text{-}tpy)_2]^{2+}$ (M = Fe, Ru, Os), might arise from displacement of anions and/or solvent molecules from the electrode surface since film formation on the electrode should result in a decrease in frequency even if the film is viscoelastic. The decreases in frequency on the subsequent cathodic scans from −0.70 V are considered to result from the predominance of the frequency decrease associated with film deposition over the frequency increase associated with the ejection of anions and/or solvent molecules.

In order for the frequency to increase on the initial cathodic scan, indicating anion and/or solvent ejection, an adsorbed or deposited layer must be present on the electrode surface. To determine whether this was the case, a clean Pt electrode was immersed into a 0.10 M TBAP/AN solution containing 0.5 mM $[Cr(v\text{-}tpy)_2](PF_6)_3$, washed with pure AN, and then placed in pure 0.10 M TBAP/AN solution containing no $[Cr(v\text{-}tpy)_2]^{3+}$. Upon potential cycling a small, but clearly visible, voltammetric response due to $[Cr(v\text{-}tpy)_2]^{3+}$ was observed. Therefore, some $[Cr(v\text{-}tpy)_2]^{3+}$ appears to be adsorbed onto the electrode surface prior to the application of cathodic potentials where electropolymerization ostensibly occurs. It is also worth noting that $[Cr(v\text{-}tpy)_2]^{3+}$ is different from the complexes described above in that it undergoes two redox processes prior to electropolymerization, and the processes associated with the maintenance of charge neutrality (i.e., anion expulsion) within the adsorbed layer may give rise to the above-mentioned behavior.

The increase in frequency upon reduction became significant with continuous potential scanning (Figure 2b), since the amount of ejected anions and/or solvent molecules increased with increasing coverage of the film on the electrode. Furthermore, the frequency decreased slightly in the anodic potential scans from −1.75 to −1.20 V and then exhibited a more marked decrease upon scanning to more positive potentials with the largest changes coinciding with the voltammetric waves. This suggests that although in this case there is some electropolymerization during the anodic scan, most of the decrease in frequency is likely associated with the incorporation of anions (to maintain charge neutrality) and/or solvent molecules.

$[Co(v\text{-}tpy)_2]^{2+}$. We have previously reported, in detail, on the electropolymerization behavior of this material and on the properties of the resulting electropolymerized films.[11] In the present case, we address changes in mass concurrent with electropolymerization and redox transformations of the film on the basis of EQCM results. Parts a and b of Figure 3 present the CV and potential−frequency curve, respectively, for an electrode in contact with a 0.1 M TBAP/AN solution containing 0.5 mM $[Co(v\text{-}tpy)_2]^{2+}$ over the potential range from 0 to −1.90 V. The initial scan exhibits a metal-localized ($Co^{II/I}$) wave at about −0.70 V and a ligand-localized wave at −1.70 V. Upon

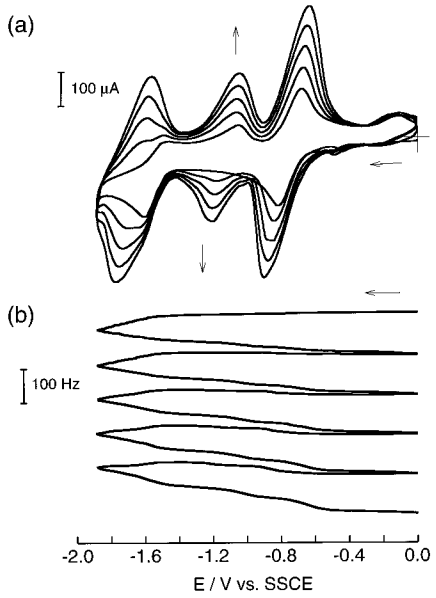

Figure 3. Typical cyclic voltammogram (a) and frequency−potential curve (b) for a quartz crystal electrode (Pt) in a 0.10 M TBAP/AN solution containing 0.5 mM $[Co(v\text{-}tpy)_2](PF_6)_2$ at 100 mV s^{-1} (five consecutive scans).

continued potential scanning, two new waves appear at ca. −0.03 and −1.1 V. These have been ascribed to the generation of $[Co(N,N',N''\text{-}v\text{-}tpy)(N,N'\text{-}v\text{-}tpy)(AN)^{3+/2+}$ and $^{2+/1+}]$ ($[Co(v\text{-}tpy)_2(AN)]^{3+/2+}$ and $^{2+/1+}$), which has partial displacement of the terpyridine ligand(s) and coordination of an acetonitrile molecule(s).[13] Upon continued potential cycling there was polymer deposition, and the frequency changed in a manner similar to that exhibited by $[M(v\text{-}tpy)_2]^{2+}$ (M = Fe, Ru, Os). Specifically, there was a large decrease in frequency starting at about −1.50 V on the cathodic scans, and the decrease continued to this same potential even after switching of the potential into the anodic direction. Since the decrease in frequency proceeded at almost the same rate in this potential region as in that where reduction of the vinylterpyridine ligand takes place, the decrease was considered to arise mainly from electropolymerization of $[Co(v\text{-}tpy)_2]^{2+}$. Continued successive scanning led to the appearance of shoulders in the frequency−potential curve at ca. −0.9 and −1.2 V on the cathodic scans and ca. −0.7 and −1.0 V on the anodic scans. These values correspond to the formal potentials of the $[Co^{II/I}(v\text{-}tpy)_2]^{2+/1+}$ and $[Co^{II/I}(v\text{-}tpy)_2(AN)]^{2+/1+}$ processes, respectively. These changes in frequency are ascribed to incorporation and ejection of anions and/or solvent molecules through the film/solution interface to maintain charge neutrality and appropriate solvation within the film.

$[Ni(v\text{-}tpy)_2]^{2+}$. At negative potentials, this material exhibited two waves centered at −1.20 and −1.57 V corresponding to Ni(II/I)-localized and vinylterpyridine-localized redox processes, respectively (Figure 4a).[13] Upon scanning to negative potentials, the frequency decreased significantly from ca. −1.1 to −1.4 V and then reached an almost steady state (Figure 4b). After sweep reversal at −1.80 V, the frequency remained virtually constant up to −1.30 V and then gradually decreased during completion of the anodic scan to 0 V. From the fifth potential scan (see asterisk) during continuous scanning, the frequency increased during the cathodic sweeps from −1.0 V and decreased in the subsequent anodic sweeps. At first this would appear to be an unanticipated result, since the decrease in frequency would indicate electropolymerization which would suggest that the first reduction corresponds to a ligand (and not metal) based process. However, these observations can be

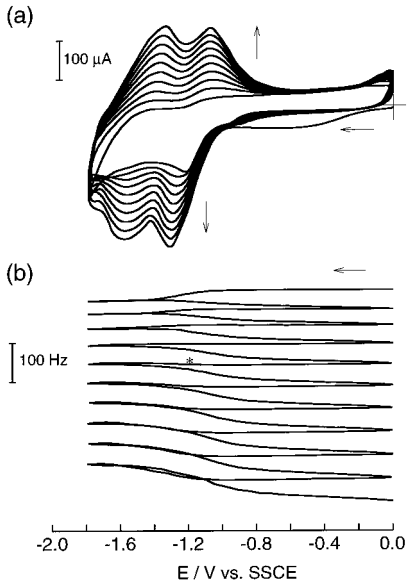

Figure 4. Typical cyclic voltammogram (a) and frequency−potential curve (b) for a quartz crystal electrode (Pt) in a 0.10 M TBAP/AN solution containing 0.5 mM $[Ni(v\text{-}tpy)_2](PF_6)_2$ at 100 mV s^{-1} (10 consecutive scans). The asterisk (*) denotes the fifth scan.

rationalized by considering that when the potential was scanned to −1.40 V, electropolymerization still proceeded although the efficiency of the polymerization was lower than when the potential was scanned to −1.80 V. Thus, although formally the first reduction wave corresponds to a metal-localized process, there appears to be some electron density on the ligand from about −1.0 V. This could arise from π back-bonding interactions (metal to ligand) since the electron goes into a metal-based π orbital which is capable of back-donation to the ligand's π^* orbital. Therefore, the decrease in frequency from about −1.0 V observed during the initial scans may be ascribed to accumulation of the polymer film onto the electrode. This behavior is different from that observed for $[M(v\text{-}tpy)_2]^{2+}$ (M = Fe, Ru, Os). In addition, once there is material deposited (even for thin films), further reduction from about −1.40 V causes a decrease in the frequency due to further polymerization and an increase in the frequency due to anion and/or solvent ejection from the film/solution interface to maintain charge neutrality and appropriate solvation within the film, resulting in virtually no net changes in frequency during the initial cathodic scan from −1.4 V. These differences may be rationalized by considering that ligand reduction in this case takes place at significantly more negative potentials (and thus the film is in the reduced form for a smaller fraction of the time) and might also reflect differences in electropolymerization rates. As the film's thickness increased, the increase in the frequency caused by ejection of anions and/or solvent molecules from the film is greater than the decrease in frequency caused by further polymerization (due to a slower rate of polymerization), thereby resulting in an overall increase in frequency.

Film Thickness and Resistance Parameter. Next, we studied changes in the resistance parameter of the electrical equivalent circuit for a quartz crystal resonator after electropolymerization (to different coverage values) of the various $[M(v\text{-}tpy)_2]^{n+}$ complexes. As previously mentioned, it is important to establish the main factor(s) leading to the frequency changes observed during electropolymerization. It was thought that electropolymerization of the $[M(v\text{-}tpy)_2]^{n+}$ complexes could cause large changes (especially at high coverage values) in the film's properties such as viscoelasticity which would lead to

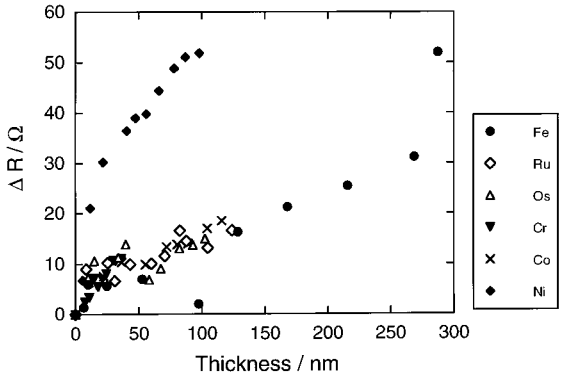

Figure 5. Dependence on polymer film thickness (calculated from surface coverage) of the resistance parameter of the electrical equivalent circuit for a quartz crystal resonator in contact with a 0.10 M TBAP/AN solution containing 0.5 mM $[M(v\text{-}tpy)_2](PF_6)_n$ (M = Fe(II), Ru(II), Os(II), Cr(III), Co(II), and Ni(II) and $n = 2$ for Fe, Ru, Os, Co, and Ni or $n = 3$ for Cr) at 100 mV s^{-1}.

changes in the resistance. Figure 5 shows the dependence of ΔR (defined as the difference in resistance after every potential scan at 100 mV s^{-1} and the initial resistance (prior to polymerization)) as a function of the thickness of the electropolymerized film on the crystal resonator in a 0.1 M TBAP/AN solution containing 0.5 mM of the $[M(v\text{-}tpy)_2]^{n+}$ complex. The thicknesses were calculated from the measured surface coverages of the electrodeposited films of the $[M(v\text{-}tpy)_2]^{n+}$ complexes assuming a diameter of 14 Å for each complex molecule (estimated by using van der Waals radii). A similar value could also be obtained from the X-ray crystal structure of $[Ru(bpy)_3](PF_6)_2$.[36] The surface coverages were measured in pure TBAP/AN solution after each potential scan in a solution containing the $[M(v\text{-}tpy)_2]^{n+}$ complex. As can be seen in Figure 5, the resistance of all the electrodeposited films examined increased as the film thickness increased. These increases in the resistance parameter may be a manifestation of increases in the viscoelasticity, surface roughness of the film, or the thickness of the film. This suggests that calculations of mass changes from the changes in the frequency due to polymerization by continuous potential cycling (as mentioned in the previous section) may not be straightforward, particularly at high coverage values.

The changes in the resistance parameter for electropolymerized films of $[Ni(v\text{-}tpy)_2]^{2+}$ were significantly larger than those for the other complexes, indicating that films derived from this material might be more viscoelastic and/or their surfaces rougher than the other ones (see Figure 5). Further, with the exception of films derived from $[Ni(v\text{-}tpy)_2]^{2+}$, the viscoelasticity and/or roughness of the polymer films derived from the other $[M(v\text{-}tpy)_2]^{n+}$ complexes were quite similar as ascertained from variations in the resistance parameter with surface coverage (Figure 5).

However, it should be mentioned that the polymerization efficiency appeared different for each material, since the growth rates of films were different for each $[M(v\text{-}tpy)_2]^{n+}$ complex. $[Fe(v\text{-}tpy)_2]^{2+}$ and $[Cr(v\text{-}tpy)_2]^{3+}$ exhibited the highest and lowest polymerization rates, respectively. These results are in good accordance with those obtained by EQCM methods, where $[Fe(v\text{-}tpy)_2]^{2+}$ and $[Cr(v\text{-}tpy)_2]^{3+}$ exhibited the largest and smallest overall decreases in frequency, respectively, upon continuous potential cycling. These differences in polymerization efficiencies could be due, at least in part, to differences in the potentials at which the v-tpy ligands are reduced (and the resulting differences in time during which the ligands are reduced and thus ostensibly most able to polymerize). Con-

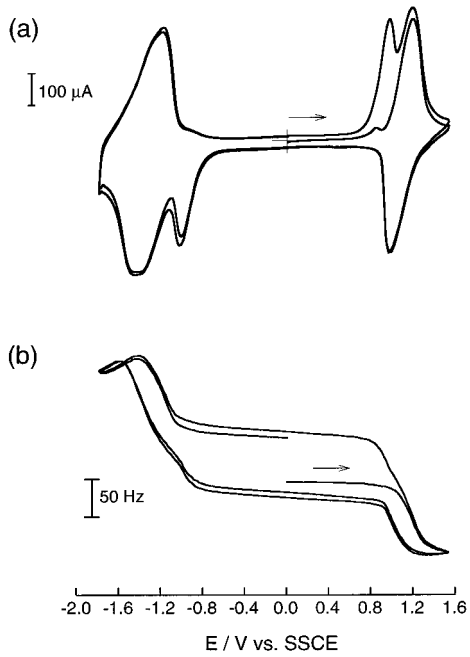

Figure 6. Typical cyclic voltammogram (a) and (b) frequency−potential curve of a poly-$[Fe(v\text{-}tpy)_2]^{2+}$ film on a quartz crystal electrode (Pt) in a 0.10 M TBAP/AN solution at 50 mV s^{-1}. Potential scanned between +1.55 and −1.80 V vs SSCE.

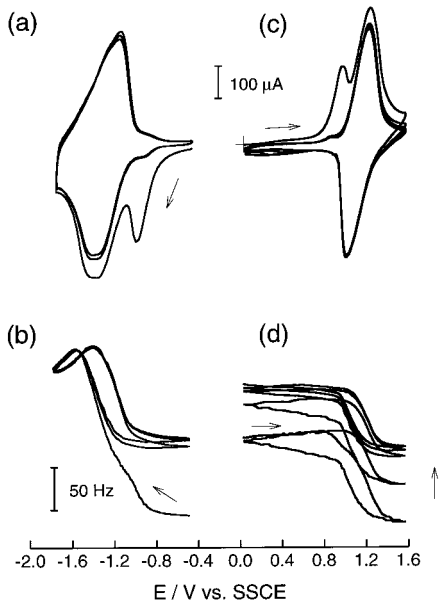

Figure 7. Typical cyclic voltammograms (a, c) and frequency−potential curves (b, d) of a poly-$[Fe(v\text{-}tpy)_2]^{2+}$ film on a quartz crystal electrode (Pt) in a 0.10 M TBAP/AN solution at 50 mV s^{-1}. Potential scanned between −0.50 and −1.80 V vs SSCE (a, c) and between 0 and +1.55 V (b, d).

sistent with this is the fact that the Fe and Cr complexes, which represent the two extremes of polymerization rates, have the most positive (Fe) and the most negative (Cr) formal potentials for the ligand-based reductions. Although π back-bonding interactions could play some role, we do not believe them to be dominant since if that was the case, the Os and Ru (and not the Fe) complexes should exhibit the highest electropolymerization rates.

Mass-Transfer Process of Poly-$[M(v\text{-}tpy)_2]^{n+}$-Modified Electrodes. We have previously studied the electrochemical properties as well as the electropolymerization processes of poly-$[M(v\text{-}tpy)_2]^{n+}$-modified electrodes using cyclic voltammetry.[10−13,15] Here, we examine the mass-transfer process coupled to the redox events of poly-$[M(v\text{-}tpy)_2]^{n+}$ films in a 0.10 M TBAP/AN solution using the EQCM technique. However, since the resistance parameter of the electrical equivalent circuit of the poly-$[M(v\text{-}tpy)_2]^{n+}$-coated quartz crystals changed with potential scanning (especially at higher coverages), the analysis of the data must be done with care and principally from a qualitative standpoint.

Poly-$[M(v\text{-}tpy)_2]^{2+}$ (M = Fe, Ru, Os). Since these polymer films exhibited quite similar CV and frequency responses as a function of the applied potential, results for poly-$[Fe(v\text{-}tpy)_2]^{2+}$ are shown here as representative of this group. Figure 6 shows (a) the CV and (b) the frequency−potential curve for a poly-$[Fe(v\text{-}tpy)_2]^{2+}$-modified electrode. The two ligand-based reduction waves present during the electropolymerization and centered at −1.24 and −1.41 V are now almost merged together and appear as a broadened peak centered at about −1.3 V. The wave centered at about +1.10 V is due to the metal-based Fe(II/III) oxidation (Figure 6a).

On an initially positive-going scan, a small peak was observed at +0.85 V, just before the peak corresponding to the Fe(II/III) oxidation at +1.1 V. On the subsequent potential cycle (scanning out to −1.80 V), this peak was dramatically enhanced, giving rise to a very sharp and well-defined peak that we ascribe to charge-trapping effects (Figure 6a). On the other hand, if the potential was continuously scanned between 0 and +1.55 V, the enhancement of the peak was not observed (Figure 7c). The analogous process can also be observed on cathodic sweeps where the presence of charge-trapping peaks is apparent at potentials just prior to the ligand-based reduction processes centered at about −1.30 V (Figure 7a). Such behavior is typical of charge-trapping processes and has been previously described by Murray and co-workers in the case of spatially segregated bilayer coatings on an electrode.[1,2,17,18] As mentioned earlier, charge trapping in spatially segregated bilayer films arises because the outer layer of the coating can only make electronic contact with the electrode via the inner layer. That is, since the isolated domains lack a direct pathway to the electrode, they can only be oxidized or reduced via a domain that can directly transfer charge to the electrode. Although the systems examined here do not possess a bilayer structure, the films prepared by electropolymerization of $[M(v\text{-}tpy)_2]^{2+}$ complexes behave in a fashion similar to the bilayer systems. Similar charge-trapping phenomena have previously been observed for redox polymer coatings derived from a single monomer.[7] The feature that is common to the presence of charge-trapping peaks in both situations is the existence of two well-separated redox processes (so that the conductivity is virtually zero between the two waves) that can mediate the oxidation (reduction) of domains that become "trapped" due to kinetic limitations in the rate of electron transfer.[2,37]

As mentioned above, no charge-trapping peak appeared on the first anodic scan since virtually no charge had been trapped as the potential scan was initiated at 0 V. After the second anodic scan from −1.80 to +1.55 V, a well-defined charge-trapping peak was evident. The charge associated with this peak likely arises from isolated domains within the polymer that were not oxidized at −1.0 V (where the nonisolated domains were oxidized). These isolated sites could be oxidized by mediation through the Fe(II/III) couple in nonisolated domains within the polymer at potentials just prior to +1.10 V (Figures 6a and 7c) where there is a significant enhancement of the conductivity, and due to the very large overpotential, the trapped sites are rapidly discharged. In the case where the potential was continuously scanned between 0 and +1.55 V, the charge-

trapping peak was absent since the v-tpy ligands within the polymeric film in both isolated and nonisolated domains were not reduced. Hence, there could be no trapped charge.

In Figure 6a, a similar charge-trapping peak can be seen on the cathodic scan at ca. −1.0 V, which is just prior to the peak corresponding to reduction of the v-tpy ligands within the polymer. If the potential was scanned from −0.45 to −1.80 V for a freshly prepared film or for a film whose potential was not cycled past the Fe(II/III) couple, the charge-trapping peak on the cathodic scan at −1.0 V was not observed. If the film underwent the metal-centered (Fe(II/III)) oxidation, the charge-trapping peak appeared at −1.0 V. These observations can be explained in an analogous fashion to that described above. In this case there would be Fe(III) centers that were not reduced during the cathodic scan (at ca. +1.0 V) and were thus trapped in the isolated domains. These centers could then be discharged by mediation through the ligand-based reductions of the polymer giving rise to the sharp prepeak at about −1.0 V.

The frequency response (Figure 6b) obtained concurrently with the voltammetric scan supports the existence of isolated domains within the film. As can be seen in Figure 6b, the frequency−potential curve qualitatively appears to be of the anion-exchange type. That is, the frequency decreased during oxidative processes (for both ligand and metal-localized), indicating anion incorporation into the film as well as possible changes in solvation. However, it should be noted that whereas the frequency returned to near the initial value at 0 V after the first anodic scan (as well as for continuous scans between 0 and +1.55 V), it increased by ca. 65 Hz at 0 V compared with the initial value, when the cathodic scan was extended to −1.80 V. Further, there was a significant increase in frequency (Figure 7b) upon reduction of the ligand from −0.80 V followed by a subsequent decrease in frequency upon oxidation. However, the frequency did not return to the initial value after the oxidation reaction (ligand-based) but rather was about 75 Hz higher. These differences in frequency can be ascribed, at least in part, to differences in mass arising from the trapped charge since less anions and solvent are incorporated within the film.

An estimate of the amount of charge trapped and the number of solvent (acetonitrile) molecules involved can be obtained by combining electrochemical and EQCM measurements. From integration of the area (charge) under the reduction wave due to "untrapping" (i.e., the prepeak), we estimate that about 6.3 $\times$ 10^{-9} mol cm^{-2} of charge is released, which corresponds to about 34% of the surface coverage of Fe complex. Assuming that the untrapping results in the incorporation of an equal number of perchlorate anions (so as to maintain charge neutrality), that the film morphology does not change and that the Sauerbrey equation[21] can be applied, it is found that incorporation of the anions should lead to a change in frequency of about 35 Hz. Since the total frequency change was 75 Hz, this would suggest that the additional difference in frequency of 40 Hz is due to incorporation of acetonitrile solvent. Making the same assumptions as above, we calculate that about three solvent molecules are incorporated per perchlorate anion.

If the potential was continuously cycled between 0 and +1.55 V, a steady-state response in the frequency was achieved after about two scans (Figure 7d). A similar steady-state response in the frequency was obtained upon potential cycling between −0.45 and −1.80 V (Figure 7b) for a freshly polymerized film and for a film that had undergone potential cycling but where the potential on the last anodic scan was reversed prior to the metal-localized oxidation.

A hysteresis loop in the frequency−potential scan was observed at potentials between −1.51 and −1.80 V (Figures 6b and 7b). Since there was a decrease in frequency in the cathodic sweep, this implies that there was a mass increase that we ascribe to insertion of a cation (and perhaps solvent) upon reduction of the ligand site. This process is clearly kinetic in nature since the hysteresis loop became smaller and finally was not observed as the potential scan rate was progressively decreased. The cation insertion presumably resulted from slow kinetics of anion and/or solvent ejection in order to maintain charge neutrality and the appropriate solvation within the film. This could arise from changes in the morphology of the film (see discussion below) and/or other changes in the films' properties.

From these results, the following microscopic picture is proposed. In the anodic sweep following the ligand-centered reduction (ca. −1.2 V) not all ligand sites are reoxidized, and consequently not all the anions and/or solvent molecules are reincorporated. (This represents the charge-trapping step and gives rise to an increase in frequency (see the difference in frequency at 0 V in Figure 6b).) These trapped sites are discharged in the subsequent anodic sweep at potentials just prior to the metal-based oxidation, giving rise to a rapid reincorporation of anions and/or solvent molecules to maintain charge neutrality and appropriate solvation within the film. There are also additional anions and/or solvent molecules incorporated in order to balance the subsequent positive charge associated with the oxidation of the metal centers from M(II) to M(III). In a manner analogous to the ligand-based reductions, not all M(III) sites are rereduced. (This represents the charge-trapping step in the cathodic sweep.) These trapped sites are discharged in the subsequent cathodic sweep at potentials just prior to the ligand-based reduction (ca. −1.0 V), giving rise to a rapid ejection of anions and/or solvent molecules to maintain charge neutrality.

These processes may be caused, at least in part, by changes in the film morphology. For example, the film may shrink upon ligand reduction and associated anion and/or solvent ejection. This would especially be the case after the second ligand-based reduction where the film would ostensibly be neutral, thus giving rise to significant changes in ionic content and extent of solvation. Such changes could present kinetic barriers to the efficient uptake of anions and/or solvent molecules upon reoxidation, leaving some sites in their reduced form and thus giving rise to charge trapping in what would ostensibly represent electrochemically isolated microdomains. These trapped sites would then be discharged at potentials in the vicinity of the metal-based oxidation (due to the enhanced conductivity of the film at these potentials and the very high overpotential present), resulting in the charge-trapping peak, and accompanied by the insertion of anions necessary to maintain charge neutrality. Moreover, the combination of this charge-trapping peak along with the metal-based oxidation and the accompanying additional insertion of anions and/or solvent molecules would clearly result in abrupt changes in the ionic contents and degree of solvation within the film, thus likely leading to an expansion of the film.

A qualitatively similar situation would be applicable for the metal-based oxidation processes where part of the metal centers are trapped in the M(III) oxidation state and are subsequently discharged at potentials just prior to the ligand-localized reduction.

The proposed mechanism of charge trapping for single-component coatings is further supported by admittance measurements of poly-$[M(v\text{-}tpy)_2]^{2+}$-coated quartz crystal resonators (M = Fe, Ru, Os). Parts a and b in Figure 8 depict respectively a

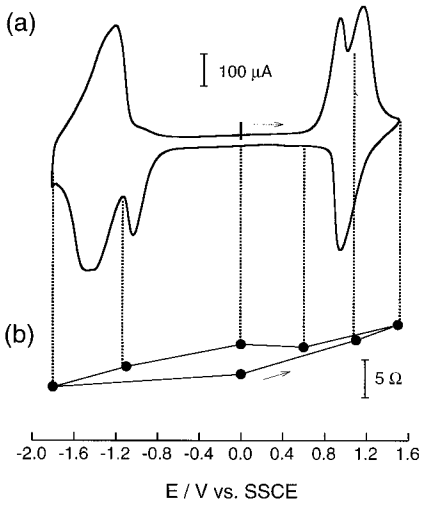

Figure 8. Steady-state cyclic voltammogram at 100 mV s^{-1} (a) and potential dependence of the resistance parameter of the electrical equivalent circuit (b) for a poly-$[Fe(v\text{-}tpy)_2]^{2+}$ film-coated quartz crystal resonator in contact with a 0.10 M TBAP/AN.

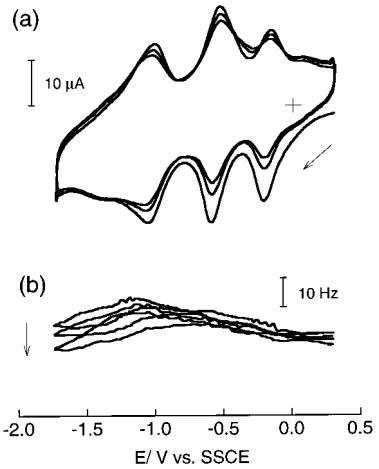

Figure 9. Typical cyclic voltammogram (a) and frequency−potential curve (b) of a poly-$[Cr(v\text{-}tpy)_2]^{3+}$ film on a quartz crystal electrode (Pt) in a 0.10 M TBAP/AN solution at 50 mV s^{-1}.

typical steady-state CV (a) and resistance parameter (b) of the electrical equivalent circuit for a poly-$[Fe(v\text{-}tpy)_2]^{2+}$-coated quartz crystal resonator in a 0.1 M TBAP/AN solution. As can be seen in Figure 8b, both metal- and ligand-localized reductions (i.e., Fe(III) → Fe(II) and tpy° → $tpy^{\bullet -}$) cause a decrease in the resistance (ca. 2 Ω), presumably corresponding to a shrinkage of the film, while both metal- and ligand-localized oxidations (i.e., Fe(II) → Fe(III) and $tpy^{\bullet -}$ → tpy°) cause an increase in the resistance parameter (ca. 2 Ω), corresponding to a swelling of the film. Similar changes in the resistance parameter were also observed for poly-$[Ru(v\text{-}tpy)_2]^{2+}$ and poly-$[Os(v\text{-}tpy)_2]^{2+}$ films. Here it should be noted that the contribution of the changes in the resistance parameter (as described above) to the changes in frequency observed upon the redox reaction of the poly-$[Fe(v\text{-}tpy)_2]^{2+}$ film are considered to be small, since the observed changes in the resistance parameter were small. Therefore, although a quantitative analysis of the changes in mass (as derived from frequency changes) was difficult, qualitative analyses were considered to be reliable.

Poly-$[Cr(v\text{-}tpy)_2]^{3+}$. Figure 9 shows (a) the CV and (b) the frequency−potential curve for a poly-$[Cr(v\text{-}tpy)_2]^{3+}$-coated quartz crystal resonator. It should be noted that in this case the current (at most ca. 20 μA) and the overall changes in frequency (ca. 15 Hz; maximum−minimum over the potential range scanned) were much smaller than those of $[M(v\text{-}tpy)_2]^{2+}$ films (100−400 μA and 140−270 Hz, for M = Fe, Ru, Os) due to the lower coverage values for films of $[Cr(v\text{-}tpy)_2]^{3+}$, as previously mentioned. Similar to the other polymer films examined, the increase or decrease in frequency during cathodic and anodic scans over the potential range from +0.3 V to ca. −1.1 V is considered to be a manifestation of ejection or incorporation of anions and/or solvent from or into the polymer film, respectively.

In the cathodic scan and over the potential range from ca. −1.1 to −1.75 V the decrease in frequency is likely due to the insertion of cations and/or solvent into the film to compensate the charge generated by the Cr/ligand-localized redox reaction, since this produces a polymeric film with a net negative charge so that the incorporation of cations would be required to maintain charge neutrality. The reverse processes would account for the frequency decrease in the corresponding anodic sweep.

In Figure 9b it can also be noted that the potential at which the maximum frequency is attained, from either the cathodic or anodic directions, shifted to more positive values with continuous potential scanning. In addition, all peak heights (in the voltammetric scans) and the overall frequency changes decreased with continuous potential scanning. This behavior could be caused by the formation of electrochemically inactive ion pairs between $[Cr(v\text{-}tpy)_2]^{n+}$ and $(ClO_4^-)_n$ accumulated in the film with continuous potential cycling, resulting in a decrease in the overall frequency. Further, since the formation and accumulation of ion pairs would result in a decrease in the number of mobile anions in the film, the number of cations (presumably tetra-*n*-butylammonium cations from the supporting electrolyte) increased and became the majority charge-carrying species moving through the film/solution interface. The increase in the cation concentration within the film would, in turn, result in a positive shift of the potential giving the maximum frequency.

Results of admittance measurements also support this proposed mechanism. The resistance parameter of a poly-$[Cr(v\text{-}tpy)_2]^{3+}$-coated quartz crystal resonator decreased significantly (ca. 150 Ω) with two potential cycles and then reached a steady-state value. In general, a decrease in the resistance parameter indicates an increase in the rigidity and/or shrinking of the film, causing an increase in frequency. However, in the case of poly-$[Cr(v\text{-}tpy)_2]^{3+}$, the successive potential scans caused a decrease in both the resistance parameter and frequency. If there was no contribution from changes in mass to the film morphology (thus resistance parameter) and the rigidity of the film increased independently with successive potential sweeps, then the frequency should increase. Thus, these results suggest that the ions incorporated into the film with potential scanning led to an increase in the rigidity of the film and/or film shrinkage.

Poly-$[Co(v\text{-}tpy)_2]^{2+}$. The CV and frequency−potential curve for a poly-$[Co(v\text{-}tpy)_2]^{2+}$ film over the potential range from +0.6 to −1.9 V are shown in Figure 10, a and b, respectively. In the CV there are four peaks centered at +0.25, −0.80, −1.18, and −1.68 V, corresponding to $[Co^{III/II}(v\text{-}tpy)_2]$, $[Co^{II/I}(v\text{-}tpy)_2]$, $[Co^{II/I}(v\text{-}tpy)_2(AN)]$, and ligand-based reduction, respectively. At potentials around −0.03 V, however, a peak corresponding to $[Co^{III/II}(v\text{-}tpy)_2(AN)]$ was not observed. This may be due to less formation of $[Co(v\text{-}tpy)_2(AN)]$ under the conditions examined as well as to the small electron self-exchange rate of $[Co^{III/II}(v\text{-}tpy)_2(AN)]$. In addition, the peak for $[Co^{II/I}(v\text{-}tpy)_2(AN)]$ at −1.18 V appeared to be somewhat broader than those of

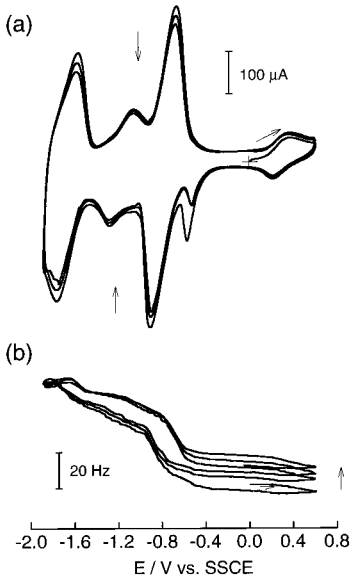

Figure 10. Typical cyclic voltammogram (a) and frequency−potential curve (b) of a poly-$[Co(v\text{-}tpy)_2]^{2+}$ film on a quartz crystal electrode (Pt) in a 0.10 M TBAP/AN solution at 100 mV s^{-1}.

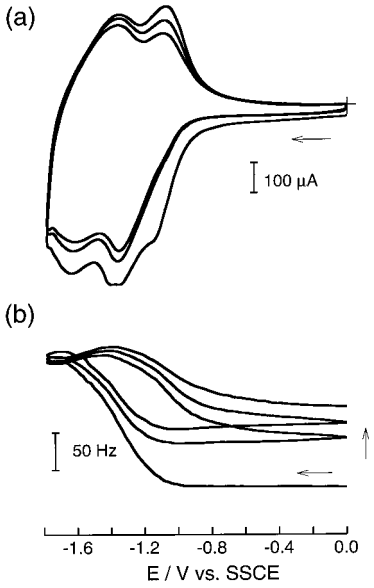

Figure 11. Typical cyclic voltammogram (a) and frequency−potential curve (b) of a poly-$[Ni(v\text{-}tpy)_2]^{2+}$ film on a quartz crystal electrode (Pt) in a 0.10 M TBAP/AN solution at 50 mV s^{-1}.

$[Co^{II/I}(v\text{-}tpy)_2]$. Similar phenomena were observed in our previous report.[11]

Similar to the other complexes examined, the changes in frequency, shown in Figure 10b, suggest that the film is of the anion-exchange type. The frequency increased and decreased (ca. 17 Hz) upon reduction and oxidation, respectively, at ca. +0.25 V for the $[Co^{III/II}(v\text{-}tpy)_2]$ process, but much larger changes (ca. 45 Hz) were observed at ca. −0.80 V for the $[Co^{II/I}(v\text{-}tpy)_2]$ process. This is likely a manifestation of a kinetic effect arising from the significant differences in the charge propagation rate (apparent diffusion coefficient) for $[Co^{III/II}(v\text{-}tpy)_2]$ vs $[Co^{II/I}(v\text{-}tpy)_2]$ with the former being significantly lower than the latter. Frequency changes associated with reduction and oxidation of the $[Co^{II/I}(v\text{-}tpy)_2(AN)]$ couple (at ca. −1.18 V) took place at a much slower rate than for the $[Co^{II/I}(v\text{-}tpy)_2]$, and again, this is likely a reflection of kinetic effects due, in this case, to the relatively low coverage of this species. Furthermore, the frequency increased sharply upon ligand-based reduction, followed by a decrease upon further reduction, which may be caused by insertion of cations (to maintain electrical neutrality) with low mobility, resulting in the hysteresis loop that appeared from −1.77 to −1.9 V.

Here, it should be noted that continuous potential scanning caused a diminution in all the voltammetric peaks as well as an increase in the overall frequency, especially over the potential range between +0.6 and −0.6 V (Figure 10b). This suggests that some anions and/or solvent molecules may not have been reinserted back into the film upon the oxidation processes associated with $[Co^{I/II}(v\text{-}tpy)_2]$ and $[Co^{II/III}(v\text{-}tpy)_2]$, probably due to changes in the film morphology. The presence of a small, but clearly discernible, charge-trapping peak (Figure 10a) is consistent with this. Changes in the film morphology are also supported by admittance measurements of a poly-$[Co(v\text{-}tpy)_2]^{2+}$-coated quartz crystal resonator. The resistance parameter of the quartz crystal continuously decreased with continuous potential scanning (ca. 15 Ω for three scans), specifically exhibiting large decreases upon reduction of $[Co^{II/I}(v\text{-}tpy)_2(AN)]$. These results suggest that the poly-$[Co(v\text{-}tpy)_2]^{2+}$ film shrinks with potential scanning, especially following the reduction of $[Co^{II/I}(v\text{-}tpy)_2(AN)]$, due to anion and/or solvent ejection. This would, in turn, result in difficulties in the incorporation of anions and/or solvent molecules into the film upon oxidation, causing the formation of electrochemically inactive sites since their charges were not compensated.

It should be also mentioned that if the film underwent continuous potential scanning, the frequency gradually decreased and the resistance parameter gradually increased at the open-circuit potential and reached values that were close to the original ones observed before potential scanning of the modified electrode. Furthermore, this "aged" film exhibited an electrochemical response that was quite similar to that of the original film. These results suggest that the film shrinks with potential cycling and that it gradually swells back by insertion of anions and/or solvent and support the proposed mechanism for film aging. This behavior, however, is quite different to that exhibited by poly-$[Cr(v\text{-}tpy)_2]^{3+}$.

Poly-$[Ni(v\text{-}tpy)_2]^{2+}$. This film exhibited metal center-localized Ni(II/I) and ligand-based redox processes centered at −1.23 and −1.51 V, respectively (Figure 11a).[13,38] The Ni(II/I) reduction caused a large increase in frequency as did the ligand-based reduction until the potential reached −1.75 V, after which the frequency decreased (Figure 11b). On the reverse (anodic) scan, the frequency continued to decrease upon ligand oxidation and then increased until the potential reached ca. −1.4 V, after which it decreased. The frequency continued to decrease significantly through the metal-centered oxidation (I/II). Similar to the other films examined, the decrease in frequency upon ligand reduction may be due to the incorporation of cations, with small mobility, into the film, resulting in the appearance of a hysteresis loop in the frequency−potential scan. As in the previous cases where such hysteresis loops were observed, if a slower potential scan rate was used, the loop eventually disappeared, again suggesting its kinetic origin.

In addition, continuous potential cycling caused a continuous increase in the frequency between −1.40 and −1.75 V. Also, if the potential was stepped from 0 to −1.9 V, where the ligand exists in its reduced form, the frequency initially decreased by about 30 Hz within 10 s, presumably corresponding to the insertion of cations. Afterward, it gradually increased by about 130 Hz over a 20 min period followed by further increases, at a slower rate, approaching a value close to the original frequency of the bare quartz crystal. Moreover, continuous potential

scanning caused a diminution in all the peaks in the voltammogram and an increase in the overall frequency. Leaving the electrode in a 0.1 M TBAP/AN solution at open circuit after this experiment did not cause a recovery in the frequency or an increase in the electrochemical response. These observations are consistent with the ejection of anions and/or solvent molecules from the film and dissolution of the polymer film. Changes in the resistance parameter of poly-$[Ni(v\text{-}tpy)_2]^{2+}$-coated quartz crystal also support these assertions since the resistance parameter continuously decreased with successive potential scanning (ca. 50 Ω for five scans), which would correspond to a decrease in the film thickness.

Conclusions

Using the EQCM technique and admittance measurements of the resonator, the electropolymerization processes of $[M(v\text{-}tpy)_2]^{n+}$ ($M = Fe^{II}$, Ru^{II}, Os^{II}, Cr^{III}, Co^{II}, Ni^{II}) have been studied. A decrease in frequency upon ligand reduction for the complexes, $[M(v\text{-}tpy)_2]^{n+}$ ($M = Fe^{II}$, Ru^{II}, Os^{II}, Cr^{III}, Co^{II}), confirms that polymerization is initiated by reduction of the ligand. In contrast, the polymerization for $[Ni(v\text{-}tpy)_2]^{2+}$ appears to involve an ostensibly metal-centered reduction. This is rationalized by taking into account the effects of π back-bonding interactions from the metal to the ligand. The polymerization efficiencies of $[Fe(v\text{-}tpy)_2]^{2+}$ and $[Cr(v\text{-}tpy)_2]^{3+}$ were found to represent the upper and lower limits, respectively, for all the materials investigated, and these rates were correlated with the values of the potentials for the ligand-localized reductions.

The metal-centered redox processes of the polymerized $[M(v\text{-}tpy)_2]^{n+}$ films appear to be of anion-exchange type, although there appears to be some effect of cation movement on the ligand-centered redox processes—likely due to slow movement of anion and/or solvent molecules through the film/solution interface due to changes in the film morphology. A mechanism of the "charge-trapping" phenomenon for single-component coatings of poly-$[M(v\text{-}tpy)_2]^{2+}$ (M = Fe, Ru, Os) is proposed in terms of the changes in the film morphology which leads to formation of the electrochemically isolated microdomains.

Acknowledgment. This work was supported by the Office of Naval Research. F.P. acknowledges support by a NATO Fellowship.

References and Notes

(1) Abruña, H. D.; Denisevich, P.; Umaña, M.; Meyer, T. J.; Murray, R. W. *J. Am. Chem. Soc.* **1981**, *103*, 1.
(2) Denisevich, P.; Willman, K. W.; Murray, R. W. *J. Am. Chem. Soc.* **1981**, *103*, 4727.
(3) Denisevich, P.; Abruña, H. D.; Leidner, C. R.; Meyer, T. J.; Murray, R. W. *Inorg. Chem.* **1982**, *21*, 2153.
(4) Calvert, J. M.; Schmehl, R. H.; Sullivan, B. P.; Facce, J. S.; Meyer, T. J.; Murray, R. W. *Inorg. Chem.* **1983**, *22*, 2151.
(5) Murao, K.; Suzuki, K. *J. Chem. Soc., Chem. Commun.* **1984**, 238.
(6) Abruña, H. D.; Breikss, A. I.; Collum, D. B. *Inorg. Chem.* **1985**, *24*, 987.
(7) For example: Guarr, T. F.; Anson, F. C. *J. Phys. Chem.* **1987**, *91*, 4037.
(8) Baldy, C. J.; Morrison, D. L.; Elliott, C. M. *Langmuir* **1991**, *7*, 2376.
(9) Bommarito, S. L.; Lowery-Bretz, S. P.; Abruña, H. D. *Inorg. Chem.* **1992**, *31*, 495.
(10) Potts, K. T.; Usifer, D. A.; Guadalupe, A.; Abruña, H. D. *J. Am. Chem. Soc.* **1987**, *109*, 3961.
(11) Guadalupe, A. R.; Usifer, D. A.; Potts, K. T.; Hurrell, H. C.; Mogstad, A.-E.; Abruña, H. D. *J. Am. Chem. Soc.* **1988**, *110*, 3463.
(12) Arana, C.; Keshavarz, M.; Potts, K. T.; Abruña, H. D. *Inorg. Chim. Acta* **1994**, *225*, 285.
(13) Ramos Sende, J. A.; Arana, C. R.; Hernández, L.; Potts, K. T.; Keshevarz-K, M.; Abruña, H. D. *Inorg. Chem.* **1995**, *34*, 3339.
(14) Maskus, M.; Pariente, F.; Wu, Q.; Toffanin, A.; Shapleigh, J. P.; Abruña, H. D. *Anal. Chem.* **1996**, *68*, 3128.
(15) Hurrell, H. C.; Mogstad, A.-L.; Usifer, D. A.; Potts, K. T.; Abruña, H. D. *Inorg. Chem.* **1989**, *28*, 1080.
(16) Arana, C.; Yan, S.; Keshavarz-K, M.; Potts, K. T.; Abruña, H. D. *Inorg. Chem.* **1992**, *31*, 3680.
(17) Willman, K. W.; Murray, R. W. *J. Electroanal. Chem.* **1982**, *133*, 211.
(18) Pickup, P. G.; Kutner, W.; Leidner, C. R.; Murray, R. W. *J. Am. Chem. Soc.* **1984**, *106*, 1991.
(19) Buttry, D. A.; Ward, M. D. *Chem. Rev. (Washington, D.C.)* **1992**, *92*, 1355.
(20) Oyama, N.; Ohsaka, T. *Prog. Polym. Sci.* **1995**, *20*, 761.
(21) Sauerbrey, G. *Z. Phys.* **1959**, *155*, 206.
(22) Kanazawa, K. K.; Gordon, J. G. *Anal. Chim. Acta* **1985**, *175*, 99.
(23) Muramatsu, H.; Tamiya, E.; Karube, I. *Anal. Chem.* **1988**, *60*, 2142.
(24) Martin, S. J.; Granstaff, V. E.; Frye, G. C. *Anal. Chem.* **1991**, *63*, 2272.
(25) Borjas, R.; Buttry, D. A. *J. Electroanal. Chem.* **1990**, *280*, 73.
(26) Muramatsu, H.; Ye, X.; Suda, M.; Sakuhara, T.; Ataka, T. *J. Electroanal. Chem.* **1992**, *332*, 311.
(27) Beck, R.; Pittermann, U.; Weil, K. G. *J. Electrochem. Soc.* **1992**, *139*, 453.
(28) Yang, M.; Thompson, M.; Duncan-Hawitt, W. C. *Langmuir* **1993**, *9*, 802.
(29) Yang, M.; Thompson, M. *Langmuir* **1993**, *9*, 1990.
(30) Bruckenstein, S.; Fensore, A.; Li, Z.; Hillman, A. R. *J. Electroanal. Chem.* **1994**, *370*, 189.
(31) Okajima, T.; Sakurai, H.; Oyama, N.; Tokuda, K.; Ohsaka, T. *Electochim. Acta* **1993**, *38*, 747.
(32) Takada, K.; Tatsuma, T.; Oyama, N. *J. Chem. Soc., Faraday Trans.* **1995**, *91*, 1547.
(33) Oyama, N.; Tatsuma, T.; Takahashi, K. *J. Phys. Chem.* **1993**, *97*, 10504.
(34) Tatsuma, T.; Takada, K.; Matsui, H.; Oyama, N. *Macromolecules* **1994**, *27*, 6687.
(35) (a) Hughes, M. C.; Macero, D. J. *Inorg. Chem.* **1976**, *15*, 2040. (b) Hughes, M. C.; Macero, D. J. *Inorg. Chem.* **1974**, *13*, 2739.
(36) Rillema, D. P.; Jones, D. S. *J. Chem. Soc., Chem. Commun.* **1979**, 849.
(37) Gottesfeld, S.; Redondo, A.; Rubinstein, I.; Feldberg, S. W. *J. Electroanal. Chem.* **1989**, *265*, 15.
(38) Prasad, R.; Scaife, D. B. *J. Electroanal. Chem.* **1977**, *84*, 373.